

Contents lists available at ScienceDirect

Powder Technology

journal homepage: www.elsevier.com/locate/powtec



Wave propagation through submerged granular media over a wide range of fluid viscosities



Hrachya Kocharyan, Nikhil Karanjgaokar*

Mechanical Engineering Department, Worcester Polytechnic Institute, 100 Institute Rd, Worcester, MA 01609-2280, USA

ARTICLE INFO

Article history: Received 2 September 2020 Received in revised form 10 November 2020 Accepted 11 November 2020 Available online 24 November 2020

Keywords:
Granular matter
Immersed granular media
Wave attenuation
Impact loading
Wave propagation

ABSTRACT

The low-velocity impact response of 2D granular crystals immersed in various fluids over a wide range of viscosities $(1-10^6\ cP)$ was investigated. The drag effects in the immersed crystals results in significantly higher wave attenuation as compared to dry granular crystals. In order to quantify the spatial dependence of the wave decay characteristics, the coefficients of attenuation were computed for the dry granular crystals and granular crystals immersed in various fluids. The coefficient of attenuation for immersed granular crystals was significantly larger than the coefficient of attenuation for dry granular crystals. As the viscosity increased, the coefficient of attenuation also increased due to the additional drag effects followed by an unexpected decrease for the highest viscosity fluids. The ratio of kinetic energy to strain energy for immersed granular crystals decreases initially as a function of viscosity but increases again for the fluids with the highest viscosities.

© 2020 Elsevier B.V. All rights reserved.

1. Introduction

Dry granular materials are materials made of macroscopic particles acting collectively. It is well known that interactions in dry granular materials are only through individual contacts between the particles and dry granular materials have negligible cohesion, essentially meaning that they can be separated without overcoming any attractive forces [1]. However, the presence of moisture or another fluid content in the granular media can completely alter the mechanical or physical properties as well as wave dynamics of granular materials. In fact, the nature of interparticle contact interactions and resulting mechanical properties and wave characteristics of wet granular media can change significantly with various degrees of wetness or fluid content. The accurate description of how fluid content affects the properties of granular materials could have major implications on numerous real-world applications involving wet and immersed granular materials. The accurate description of the mechanics of wet/immersed granular materials is critical in many geological applications e.g. understanding the mechanics of snow avalanches [2] and rain-induced landslides [3] to predict potential avalanches/landslides and design structures to reduce disasters. The mechanics of immersed granular materials is vital in civil engineering applications and construction materials for underwater constructions [4]. The mechanics and flow of wet and immersed granular media also plays a major role in the pharmaceutical and food processing industry [5].

Depending on the degree of wetness or fluid content, four regimes with increasing fluid content can be defined in wet granular media: 1) Pendicular state, 2) Funicular state, 3) Capillary state, and 4) Submerged or immersed state. In the pendicular state for granular media, the inter-particle contact interactions are cohesive in nature as a result of the formation of fluid bridges around the individual contacts [1]. The contact interactions in the funicular and capillary state of granular media are also cohesive in nature with additional considerations due to the presence of voids in the former state and pore formation due to surface tension in the latter state. At high fluid content in granular media i.e. in the fully immersed state, cohesion is absent in the inter-particle contact interactions [6]. However there are viscous and velocitydependent effects on contact interactions in immersed granular media [7] e.g. drag on particles resulting in higher dissipation. Although there are a considerable number of studies that investigate the mechanical behavior of dry granular materials in various scenarios, the literature on wet and immersed granular materials is very limited in comparison. In the past, Tegzes et al. [8] observed that at low fluid contents dry and wet cases have identical behavior with a clear transition from continuous to avalanching flow, which lacks at higher fluid contents. Jarray et al. [9] found that the presence of secondary fluid increases the depth of flowing layers and reduces the mobility of the particles. In [10], the effects of fluid viscosity on segregation in a rotating drum were investigated and it was found that the angle of repose has a sharp increase with increasing fluid viscosity. The segregation index decreases dramatically with increasing fluid viscosity, thus higher viscosity mitigates segregation, indicating that the fluid viscosity has a huge effect on the behavior of the granular segregation. Other experiments have reported on the compaction of

^{*} Corresponding author.

E-mail addresses: hkocharyan@wpi.edu (H. Kocharyan), nkaranjgaokar@wpi.edu
(N. Karanjgaokar).

wet granular assemblies [11,12], where it was found that the surface tension of the fluid decreases the packing fraction of the assembly, whereas the characteristic compaction time was found to sharply increase with increasing surface tension [11]. An important dynamical behavior of granular materials is the segregation phenomena observed in wet granular materials. The cohesion arising due to the fluid bridges slows down the segregation in wet granular materials, it is still observed often [13,14]. However, it was found that the viscosity of the wetting fluid has a huge impact on the segregation, as the segregation is not present for high viscosity fluids [13], similarly, segregation does not appear for high fluid content [14]. While there are various specific examples for investigations on the physics of wet granular materials, in contrast, the literature investigating the mechanics of immersed granular materials is even more limited in terms of both their numbers and their scope. Most of the work on the immersed granular matter is an investigation of avalanching behavior utilizing molecular dynamics [15,16] or using rotating drums [17-19] and tiltable cells [20] and crater formation [21,22]. Another type of experiments that were of significant interest lately were submerged granular discharges through an aperture [23-25]. While the discharge of the dry granular system has a constant rate for most of the discharge process and the discharge of fluids slows down over time, it was found that the discharge rate of the submerged granular system accelerates throughout the whole discharge process [23,24]. The discharge process was found to be governed by the friction between the particles, as the discharge was slowing down for frictionless particles both in dry and submerged granular systems, was constant for dry frictional particles, and was accelerating for submerged frictional particles [23]. In the recent past, there has been a substantial interest in the investigation of granular chains embedded in the secondary medium polymer matrix [26]. In [26], the authors have found that embedding the chain in polymer matrix results in higher dissipation and reduce the force transmission through the chain, moreover, the pulse propagation speed was the smallest for the embedded chain. These works on granular media embedded in a polymer matrix can be thought of as the most extreme case of granular material in secondary viscous media. However, to the best of the authors' knowledge, there is no literature that bridges the gap between granular materials in low viscosity fluids (e.g. water) to granular materials in secondary viscous solids (e.g.: polymers). This manuscript provides a new insight into the role of the viscosity of the secondary media on the mechanics of the granular materials.

2. Experimental procedure

A schematic representation of the drop-tower based low-speed impact experimental setup is shown in Fig. 1a. It is built on a rigid fixture with adjustable perforated sidewalls, allowing the fluid to freely flow into and out of the system, which ensures the absence of any potential pressure build-ups in the system and achieves projectile velocities \sim 6 m/s. In order to be able to image the experiment, the front wall of the setup needs to be transparent, and since high-speed imaging requires a high level of light intensity, to minimize potential distortions from the bright light sources an anti-reflective coated glass (Edmund Optics) with a 93-94% transmission was used as the front wall. Since the experimental setup, which is closed from all sides, is required to be leak-proof during the low-speed impact experiment, the transparent front wall was attached to the rigid metallic fixture setup using an elastomeric sealing agent. The elastomeric sealing agent was employed at all other potential wall joints to avoid leaks during the experiments. In this work, Polyurethane (Durometer 80A, McMaster-Carr) cylindrical grains with around ½ in diameter and 1 in length were arranged into a granular crystal in a cubic arrangement as shown in Fig. 1b. The material properties such as density, elastic modulus, poisson's ratio and the coefficient of friction for the cylinderical polyurethane grains used in the granular crystals are listed in Table 1. The experimental setup has adjustable rigid sidewalls and can accommodate up to 20 columns and up to 15 rows grains of ½ in diameter. In the experiments presented in the current work, granular crystals with 15 columns and 13 rows were immersed in the various secondary fluids. The viscosity values for the various secondary fluids used in immersed granular crystals are listed in Table 2. A random, dense speckle pattern was deposited on the front face of each individual polyurethane cylindrical grain to allow for the subsequent DIC analysis for the computation of the particle kinematic and strain fields. In order to ensure the success of the proposed low-speed impact experiment for immersed granular materials, a few stringent requirements needed to be satisfied; 1) the glass front wall to be protected from huge pressure increase in fluid phase during impact loading, 2) the experiment design needs to avoid the potential bubble formation and other complications due to the interaction of the fluid with the sidewalls and 3) the secondary fluid media should not obstruct the recording of the motion of the grains. Careful experimental design, the use of perforated sidewalls, and a small gap between the front wall and cylindrical grains account for the first two

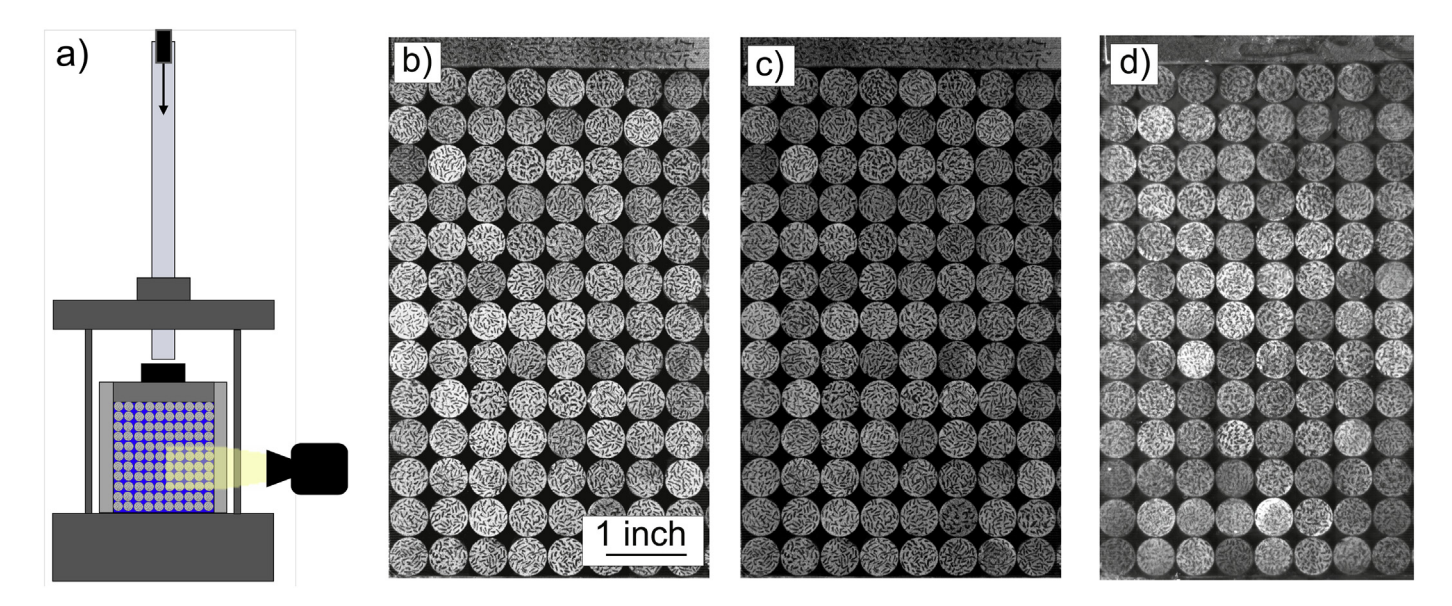


Fig. 1. a) A schematic representation of the drop-tower based experimental setup. Typical images recorded by the high-speed imaging system at 40,000 fps for the left half of the b) dry granular crystals and wet granular crystals submerged in c) transparent fluid (water) and d) opaque fluid (black transmission oil).

Table 1Material properties for the polyurethane grains used in dry and immersed granular crystals.

Material properties for polyurethane grains	
Density	1267 kg/m ³
Young's modulus	9.35 MPa
Friction coefficient	0.43
Poisson's ratio	0.49

 Table 2

 Viscosities values for various Newtonian fluids used in immersed granular crystals.

Liquid viscosities (Pa*s)	
Water	10^{-3}
80% syrup	~0.5
100% syrup	~5
Ultrasound gel	~150
Gelatin	~1000

requirements. The third requirement is a relatively trivial one for clear and semi-transparent fluids e.g. water, however, it may become a problem for opaque fluids. Fortunately, the experimental setup described in this work is versatile enough to allow impact experiments for granular crystals immersed in opaque fluids with a slight modification to the experimental approach. Typical examples of the images recorded by the high-speed imaging system for dry granular crystals and granular crystals immersed in clear and opaque fluids are shown in Fig. 1b-d. As seen in Fig. 1b-d, the speckle pattern on each individual grain can be clearly visualized in the recorded images for each case and the image quality is not compromised during a course of impact testing. The experiments with clear fluids require no additional modification and can be run directly. However, in the case of opaque fluids, the volume between the front wall and the grains can be covered in a clear and a very low friction membrane. This frictionless layer should not interfere with the vertical movement of the grains and allow the high-speed imaging system to record the motion of grains during a low-speed impact experiment. In Fig. 1d, the granular crystal is immersed in a black opaque fluid (black engine oil), however, there is an ultrasound gel in front of the grains, which allows us to record the experiments. It is important to verify that the membrane is indeed not affecting the particle motion, and it was observed that as long as there is a 2–3 mm gap between the glass and the grains and only about 1-2 mm of the grains is inside the gel, there is no detectable influence of the gel on the particle motion. In our case the opaque fluid was oil-based with low solubility for the gel, however, a different opaque fluid requires careful choice of the membrane material. The current work will only focus on the wave dynamics of granular crystals immersed in clear, Newtonian fluids, and the experiments with the opaque fluids will be discussed in more detail in our future publications.

In the current investigation, five different fluids (water, 80%, and 100% solutions of water and corn syrup, ultrasound gel, and gelatin) with viscosities in wide 10^{-3} - 10^3 Pa^*s (1- 10^6 cP) range were used. A cylindrical projectile of 4-in. length, 1-in. diameter and about 140 g mass is falling under gravity through a hollow tube, accelerating to about 6 m/s velocity and hitting the 4 in thick sliding top wall, which deforms the grains upon impact. The additional details of the experimental procedure and the subsequent post-processing of the experimental data to determine the particle-scale kinematics and strains in the granular crystal during impact loading are provided in [27,28]. The deformation of the grains was recorded at a frame rate of 40,000 fps using an optical imaging system that includes a Photron FASTCAM SA-Z high-speed camera. The kinematics and strains fields in each individual grain in the left halve of the granular crystal were calculated using a commercial digital image correlation (DIC) software (VIC-2D from Correlated

Solutions). To facilitate the usage of DIC, a random, nonrepeating speckle pattern was spray-painted on the front face of each individual cylindrical grain. Similar to [27], the surface averaging method for displacements and strains at a pixel scale is used to calculate average displacement, strain, and velocity in each grain. The DIC analysis was performed on each grain separately and the region of interest on each grain was sub-divided into around 200 subsets. Thus, the DIC analysis provides around 200 data readings for horizontal and vertical displacements for each grain with a resolution of ~0.05-0.1 pixels and an accuracy of 0.1% for the strain fields. To take advantage of the symmetry of the system and reduce the complexity and the computational cost [27], only the image of the left half of the granular crystal was recorded during the impact experiments as seen in Fig. 1b-d. In previous experiments, it was verified that this assumption of symmetry does not result in any major difference and hence the right half of the granular crystal would have a similar impact response. The initial point of projectile impact is in the top-center of the granular crystal, which would be the rightmost column in Fig. 1b-d. A typical example of velocity calculations for granular crystal subjected to low-speed impact loading is shown in Fig. 2, where the time evolution of normalized velocity of the rightmost column of grains is plotted along with the velocity fields in all grains at five different time instances, specified in Fig. 2a. While in Fig. 2b-f the velocity fields of all grains are presented, to obtain the highest possible resolution, the DIC is performed on each grain individually, and the velocity of each grain is calculated by averaging the velocities of subsets of the grain, which as mentioned above, is averaging of close to 200 readings for each particle. The average strains (ε_{xx} , ε_{xy} , ε_{yy}) for each grain was calculated using the similar procedure on the grain-scale strain fields.

Due to the difference of refraction indices between air and e.g. water, there is an expected refraction at the interfaces of air and water, so using DIC may be accompanied by unexpected inaccuracies. There are some reports on using some modification of the DIC technique for deformation measurements of objects immersed in fluids [29] and hence a relatively simplistic uncertainty analysis was performed to investigate how much a very thin layer (~2 mm) of fluid will affect the DIC results. In this analysis, an object of known sizes with a similar pattern was placed inside the fluid at the same distance between the glass front wall as the grains and was moved inside the fluid by known distances in both horizontal and vertical directions. The subsequent DIC analysis revealed that the displacement measurements were not significantly affected by the presence of the fluid layer and the displacement uncertainty was always under 1% for both directions for all cases. Since the displacement uncertainties were relatively low, no further modifications were incorporated in the DIC analysis, and the results provided by the commercially available VIC-2D software were found to be acceptable.

3. Results and discussion

The maximum value of velocity for the polyurethane grains in the central column for dry and immersed granular crystals under lowspeed impact loading are shown in Fig. 3. As seen in Fig. 3, the spatial velocity decay as a function of the distance from the point of initial impact follows a similar trend for the different types of dry and immersed granular crystals. As seen in Fig. 3, there are two distinct regions for all dry and immersed crystals, where the spatial decay of maximum velocity follows an exponential dependence of the distance in the first region and the spatial decay of maximum velocity in the second region follows a significantly higher rate. This observation is consistent with our previous reports for dry granular crystals with different arrangements [27] and this behavior was attributed to the influence of the lateral constraints on the wave propagation, more specifically, the depth where most of the kinetic energy is concentrated depends on the lateral size of the crystal. Our previous work also indicates that this behavior for wave dynamics with two distinct regions of velocity decay was also observed for different directions in the dry crystals, which is also consistent for the experiments for various granular crystals in the current

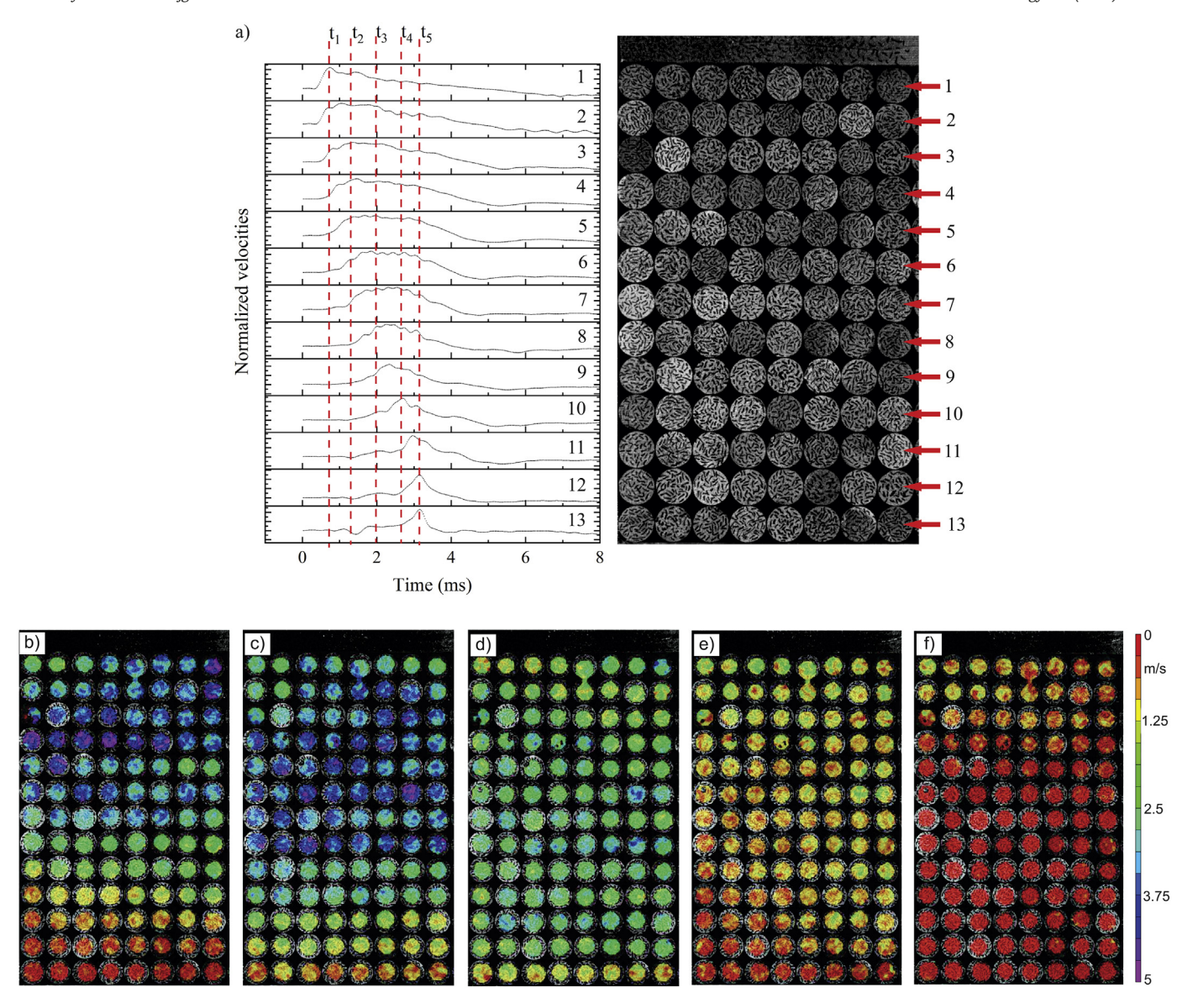


Fig. 2. a) Time evolution of velocities of the grains in the rightmost column starting with grain in 1st row to the 13th row. The velocity field for the individual grains in the left half of granular crystal immersed in water under low-speed impact loading at various instants from the time of initial impact; b) $t1 = 0.7 \, ms$, c) $t2 = 1.3 \, ms$, d) $t3 = 2 \, ms$, e) $t4 = 2.65 \, ms$ and f) $t5 = 3.1 \, ms$.

work. This proves that the wave propagation and wave decay characteristics for dry and immersed granular crystals in different fluids are quite similar. An interesting observation can be made for the granular crystal immersed in the highest viscosity fluids. As seen in Fig. 3, the region 2 with higher spatial decay rate for velocity is comparably much shorter for the granular crystals immersed in two fluids with the highest viscosities, namely ultrasound gel and gelatin. The reasons behind this difference in decay characteristics are consistent with other decay characteristics discussed below.

As mentioned earlier, the wave propagation process and the subsequent decay characteristics for dry and granular materials in fluids are quite similar. However, while there is a qualitative similarity, there is a huge quantitative difference between the two types of granular crystals. Since the spatial decay rate of the wave velocity amplitude in the region 1 follows exponential form, hence the decay rate for the experimental data presented in Fig. 3 was described using an exponential fitting in the form of $exp(-\alpha^*x)$, where α is the coefficient of attenuation or the spatial decay rate and x is the distance from the point of initial impact. The coefficient of attenuation α is the reciprocal of the

distance over which the amplitude decreases by e (Euler's constant, ~2.718) times. A similar fitting could not be performed for the region 2 for the wave velocity amplitude in the various granular crystals in Fig. 3. The trend for wave velocity amplitude in regions 2 for the different types of granular crystals does not follow an exponential decay and follows a somewhat arbitrary trend closely related to the lateral constraints imposed by the sidewalls. The actual values of the coefficient of attenuation in any particular granular crystals are influenced by a wide range of factors (such as grain size, packing, defects, grain properties, properties of secondary fluid media boundary conditions, etc.). In the experimental approach presented in the current work, the only factor that changes between the experiments for different granular crystals was the viscosity of the secondary fluid media. Thus, a comparison between the coefficient of attenuation for the various granular systems can provide a clear indication of the influence of the viscosity of the secondary fluid media on the wave attenuation. The coefficients of attenuation for various granular systems are plotted in Fig. 4, where the Fig. 4a provides a qualitative comparison between the granular crystals immersed in low viscosity fluids and the dry granular crystals on a linear

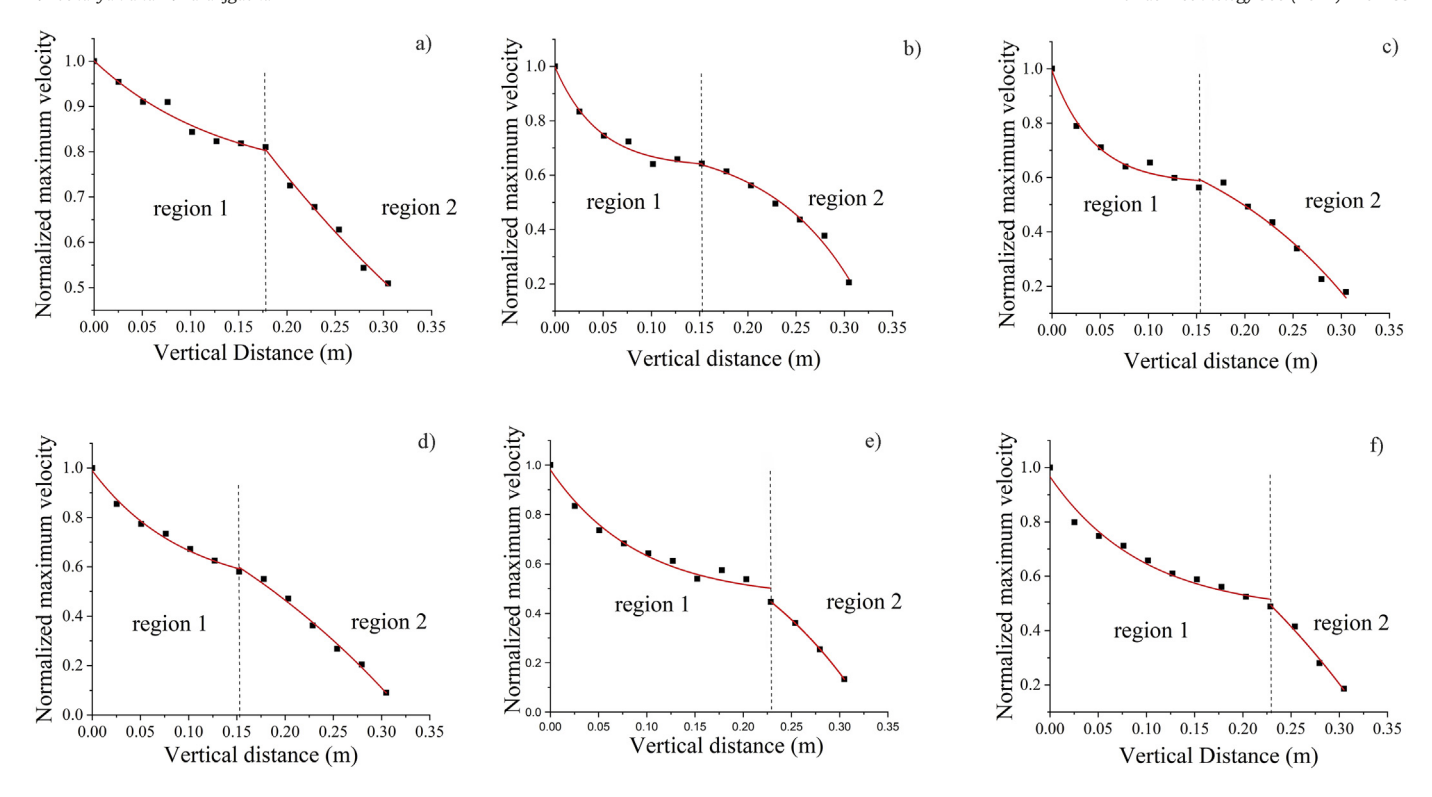


Fig. 3. The maximum amplitude of the wave velocity for the grains in the central column for (a) dry granular crystal and granular crystals immersed in (b) water, (c) 80% syrup, (d) 100% syrup, (e) ultrasound gel and (f) gelatin. The red lines in each plot indicate tentative trend-lines for the spatial dependence of the velocity decay in region 1 and region 2.

scale. The Fig. 4b provides a more comprehensive comparison between the granular crystals immersed in various fluids over a wide range of viscosity. The coefficient of attenuation for various fluid media cannot be represented on the same linear scale plot, as the inclusion of the data for the high viscosity fluids makes the low viscosity data illegible on the linear scale. It is noteworthy that the error bars due to the standard deviation from multiple experiments for each granular system are comparable to the data markers shown in Fig. 4. As seen in Fig. 4a, there is a steep increase in the coefficient of attenuation between dry and immersed granular crystals, whereas a subsequent increase of viscosity, even by powers of magnitude, results in a much smaller increase in the coefficient of attenuation. This also confirms that the presence of secondary fluid media results in a significant increase in wave attenuation as compared to dry granular crystals. This also strongly indicates that if the objective is increasing the coefficient of attenuation i.e. spatial decay of wave velocity, after a certain point, a further increase in viscosity may not result in a significant increase in wave attenuation. There is only one force acting in dry granular materials, which is the inter-particle interaction force [30], however, in immersed granular materials, there are number of new forces acting on the particles, e.g. viscous drag, inertial drag, buoyancy, the Basset force, the Magnus force [31]. While in most typical applications, especially at low speeds, we can limit the discussion to the viscous drag, all the forces mentioned act against the particles' motion, slowing them down, hence we see the sharp increase in the coefficient of attenuation in Fig. 4a. Contrary to this, increasing the viscosity of the liquid increases the magnitude of those already existing forces, thus having a smaller effect on the coefficient of attenuation. As seen in Fig. 4b, for two fluids with the highest viscosity (ultrasound gel, gelatin), there is a clear decrease in the coefficient of attenuation with an increase in viscosity. The two fluids in question have extremely high viscosities and can be considered to be soft polymers. Unfortunately, it is not trivial to explain these experimental observations for the influence of viscosity on the wave decay in immersed granular crystals. This behavior can be attributed to the fact that as the viscosity of the fluid increases, it becomes comparable to the viscosity of the particles, and the granular system starts to behave

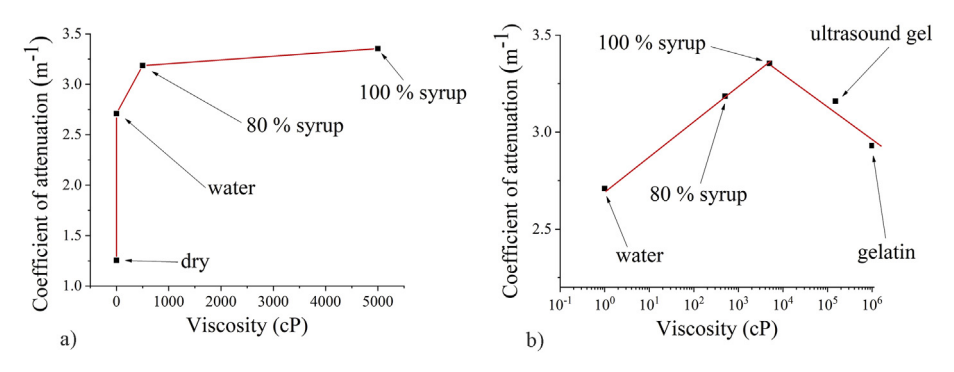


Fig. 4. The coefficient of attenuation as a function of the viscosity for (a) dry and immersed granular crystals on the linear scale and (b) immersed granular crystals on a semi-log scale.

more and more like a continuum solid media. Basically, when the viscosity of secondary fluid media such as gelatin becomes really high, it starts acting less like a viscous fluid with drag effects and more like a viscoelastic "solid" that participates in the force transmission process.

Typically the contact interaction between the grains in a granular crystal is modeled as a Hertzian contact in $F=K^*\delta^{3/2}$ form [30]. In most immersed or submerged granular systems, an additional term that accounts for the viscous drag effects is also included in the contact model. Since the current granular system consists of cylindrical grains, this viscous term can be modeled as the viscous drag on a cylindrical body in a fluid, given by [32]:

$$F = \frac{4\pi\mu aU}{\ln\left(2a/b\right) - 0.72}\tag{1}$$

where μ is the viscosity of the fluid, U is the velocity of the cylindrical object, a is the semi-length and b is the radius of the cylinder. However, this is for the case of a single long cylinder and for the case when fluid inertia is negligible. Unfortunately, the derivation of an analytical formulation for viscous drag for multiple, densely packed grains is not a trivial process that is further complicated by the difficulty of

determining fluid inertia. There are two recent reports on drag on a rod moving circularly [33] and a horizontal plate moving vertically [34] in immersed granular materials, however, the results are not applicable to our experiments. More recently, Fan et al. [25] have combined the lattice Boltzmann method (LBM) with the discrete element method (DEM) to describe the fluid-solid interaction numerically for a submerged granular system discharge case, where LBM is used for the fluid phase and DEM is used for the solid phase. The normal component of the contact force is calculated as:

$$F_{ij}^{n} = -k_n \delta_{ij}^{n} - \gamma_n \nu_{ij}^{n} \tag{2}$$

where k_n is the normal stiffness, δ_{ij}^n is the normal relative displacement of the particles in contact, γ_n is the normal coefficient of viscous dissipation and v_{ij}^n is the normal velocity of the particle. A similar approach with two components of force – one for particle-to-particle interaction, and another for the viscous dissipation could be adopted to explain for the experimental results in the current work. However, the models similar to [25] that rely on a single viscous drag term in the contact law that accounts for the drag force acting on the grain cannot explain the experimental

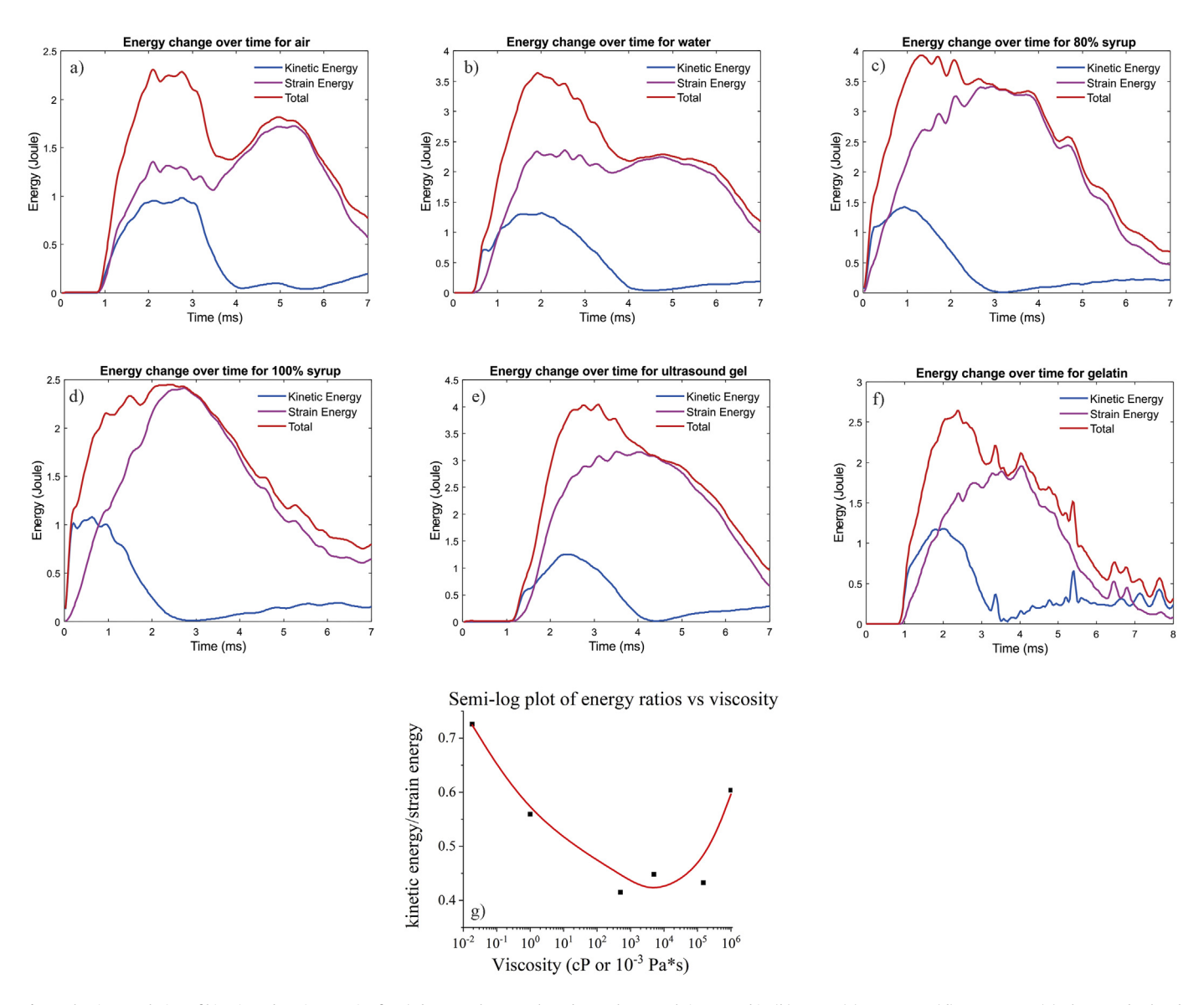


Fig. 5. The time evolution of kinetic and strain energies for a) dry granular crystals and granular crystals immersed in (b) water, (c) 80% syrup, (d) 100% syrup, (e) ultrasound gel and (f) gelatin. (g) The ratio of total kinetic and strain energies for different granular crystals are plotted as a function of viscosity on a semi-log scale.

evidence for high viscosity fluids. According to a description similar to Eq. (1), the force acting on the particle should increase indefinitely with increasing viscosity. However, as seen in Fig. 4b, initially the coefficient of attenuation increases with increasing viscosity, and this effect in wave attenuation is plateauing due to some competing mechanism. Finally, this competing effect starts dominating leading to a decrease in the coefficient of attenuation with increasing viscosity for the ultrasonic gel and gelatin. However, to the best of the author's knowledge, there are no existing models that can explain this unique phenomenon, and this raises the need for further model development. Thus, the existing DEM models for immersed granular media may have to be modified to include an additional third term in order to explain the aforementioned competing effect that reduces the wave attenuation with increase in viscosity. This third term related to the viscoelastic deformation of secondary media would probably have a viscosity dependent term with an opposite sign to the viscous term in Eq. (2).

It is well known that the kinetic energy (KE) of a moving object is highly affected by the drag of the medium, hence a decrease in kinetic energy with increasing viscosity is expected. However, the strain energy (SE) is transmitted through contacts between grains, and thus the presence of the fluid medium should have a lower impact. Since the kinematic quantities (horizontal and vertical velocity) for each grain are calculated using DIC at each time instant, the total kinetic energy (TKE) of the system can be computed by summation of the KE for each grain at any instance. Similarly, the total strain energy (TSE) can be computed using the strain data for each grain at each time instant using DIC, the nominal volume of the grain, and the effective Young's modulus [27]. In Fig. 5, the time evolution of TKE and TSE for dry and immersed granular crystals are plotted for typical low-speed impact experiments. As seen in Fig. 5, the TSE and TKE for the dry crystal are comparable, although the difference between the TSE and TKE increases with increasing viscosity. However, there is a significant decrease in the difference between kinetic and strain energies for the granular crystals immersed in fluids with the two highest viscosities. The ratio of TKE and TSE is plotted for various granular crystals in Fig. 5g. As seen in Fig. 5g, the energy ratio initially decreases, then plateaus for high viscosities and then increases again. This behavior is consistent with the results for velocity attenuation coefficients presented in Fig. 4. The drag effects due to the secondary fluid in the immersed granular systems predominantly affects the kinetic energy of the granular systems and the kinetic energy would correlate well with the spatial velocity decay in granular crystals. Thus, the initial increase in coefficient of attenuation increases as a function of fluid viscosity would result in lower TKE values and a corresponding decrease in ratio of TKE to TSE. However, for higher viscosity levels, the secondary fluid also contributes to the load transmission and counteracts the viscous drag effects Thus as the coefficient of attenuation decreases for the highest viscosity fluids i.e. the kinetic energy decay is reducing; it results in a corresponding increase in the ratio of TKE and TSE for the liquids with the highest viscosities.

As seen in Fig. 5, it is also noteworthy that although the strain and kinetic energies for dry granular crystals rise at the same time, the strain energy reaches the maximum with some delay as compared to kinetic energy for granular crystals immersed in secondary fluid media. This delay increases from around 0.7 ms for water to around 2.2 ms for 100% syrup, but then decreases again to around 1.8 ms for gelatin. The velocity of wave propagation or time-of-flight velocity, i.e. the average velocity of the peak of the initial wave traveling from the first particle to the last one increase from around 63.5 m/s for water to around 112.9 m/s for 100% syrup with a decrease to around 72.6 m/s for gelatin. Both increases and decreases in both time delay and wave propagation velocity are nonlinear and there is no clear dependence on viscosity. These observations are consistent

with literature reports for a somewhat smaller pulse propagation speed in embedded granular chains [26].

4. Conclusions

In this work, an experimental study of low-velocity impact loading of 2D granular crystals immersed in secondary fluid media over a wide range of viscosities is presented to quantitatively evaluate the role of the fluid viscosity on the wave propagation in immersed granular systems. A novel drop-tower based experimental technique was developed to investigate the wave dynamics of 2D granular crystals immersed in the different fluids that can be visualized for both clear and opaque fluids. High-speed imaging, coupled with DIC was used to calculate the kinematics of the individual particles, from which it was found that the wave propagation process in dry and immersed granular crystals is similar in nature, i.e. there are two distinct regions in the crystal, where the velocity/kinetic energy attenuation is different. However, the coefficient of attenuation was found to be strongly influenced by the viscosity of the fluid. The coefficient of attenuation of the immersed granular crystal is significantly higher than that for the dry crystal as a direct consequence of the viscous drag effects from the viscous interstitial fluid. However, a further increase in viscosity resulted in a slower growth in the coefficient of attenuation as a function of fluid viscosity due to a competing viscous effect that reduced the attenuation characteristics. This competing effect leads to plateauing of the coefficient of attenuation followed by a rather unexpected decrease as a function of viscosity. These trends are consistent with those for the ratio of kinetic and strain energies for the dry and various immersed granular crystals. Moreover, there is a time delay between kinetic and strain energy peaks due to the presence of the secondary viscous fluid medium. The viscosity of the secondary fluid medium also impacted the wave propagation velocity in immersed granular crystals. As compared to dry granular materials, the mathematical description of the mechanics of immersed granular systems is immensely more difficult due to the complexity of the physics and non-linearity of the contact interactions. Thus, this first of its kind experimental investigation establishes a clear need for model development that can explain the anomalous behavior of the immersed granular crystals over a wide range of fluid viscosity.

Declaration of Competing Interest

The authors declare that they have no known competing financial interests or personal relationships that could have appeared to influence the work reported in this paper.

Acknowledgements

The authors would also like to acknowledge the financial support through Worcester Polytechnic Institute startup funds. In particular, the authors would like to express their gratitude to the NSF-MOMS program and the program managers Dr. Qidwai and Dr. Goulbourne for the funding support through the NSF CAREER award #1845200.

References

- T. Gröger, U. Tüzün, D.M. Heyes, Modelling and measuring of cohesion in wet granular materials, Powder Technol. 133 (2003) 203–215, https://doi.org/10.1016/ S0032-5910(03)00093-7.
- [2] C. Ancey, Snow Avalanches, Geomorphol. Fluid Mech, Springer Berlin Heidelberg, Berlin, Heidelberg, 2001 319–338, https://doi.org/10.1007/3-540-45670-8_13.
- [3] R.M. Iverson, Landslide triggering by rain infiltration, Water Resour. Res. 36 (2000) 1897–1910, https://doi.org/10.1029/2000WR900090.
- [4] K.H. Khayat, M. Sonebi, Effect of mixture composition on washout resistance of highly flowable underwater concrete, ACI Mater. J. 98 (2001) 289–295, https:// doi.org/10.14359/10397.
- [5] P.-Y. Chiang, A.-I. Yeh, Effect of soaking on wet-milling of rice, J. Cereal Sci. 35 (2002) 85–94, https://doi.org/10.1006/jcrs.2001.0419.

- [6] N. Mitarai, F. Nori, Wet granular materials, Adv. Phys. 55 (2006) 1–45, https://doi. org/10.1080/00018730600626065.
- [7] M. Medved, H.M. Jaeger, S.R. Nagel, Convection in a fully immersed granular slurry, Phys. Rev. E Stat. Phys. Plasm. Fluids Relat. Interdiscip. Top. 63 (2001) 1–5, https://doi.org/10.1103/PhysRevE.63.061302.
- [8] P. Tegzes, T. Vicsek, P. Schiffer, Avalanche dynamics in wet granular materials, Phys. Rev. Lett. 89 (2002), 094301, https://doi.org/10.1103/PhysRevLett.89.094301.
- [9] A. Jarray, V. Magnanimo, M. Ramaioli, S. Luding, Scaling of wet granular flows in a rotating drum, EPJ Web Conf. 140 (2017) 1–4, https://doi.org/10.1051/epjconf/ 201714003078.
- [10] C.C. Liao, A study of the effect of liquid viscosity on density-driven wet granular segregation in a rotating drum, Powder Technol. 325 (2018) 632–638, https://doi.org/ 10.1016/j.powtec.2017.11.004.
- [11] J.E. Fiscina, G. Lumay, F. Ludewig, N. Vandewalle, Compaction dynamics of wet granular assemblies, Phys. Rev. Lett. 105 (2010), 048001, https://doi.org/10.1103/ PhysRevLett.105.048001.
- [12] S. Kiesgen de Richter, C. Hanotin, P. Marchal, S. Leclerc, F. Demeurie, N. Louvet, Vibration-induced compaction of granular suspensions, Eur. Phys. J. E. 38 (2015) 74, https://doi.org/10.1140/epje/i2015-15074-7.
- [13] A. Samadani, A. Kudrolli, Segregation transitions in wet granular matter, Phys. Rev. Lett. 85 (2000) 5102–5105, https://doi.org/10.1103/PhysRevLett.85.5102.
- [14] C.C. Liao, S.S. Hsiau, T.H. Tsai, C.H. Tai, Segregation to mixing in wet granular matter under vibration, Chem. Eng. Sci. 65 (2010) 1109–1116, https://doi.org/10.1016/j.ces. 2009.09.065.
- [15] P. Mutabaruka, J.Y. Delenne, K. Soga, F. Radjai, Initiation of immersed granular avalanches, Phys. Rev. E Stat. Nonlin. Soft Matt. Phys. 89 (2014) 1–18, https://doi.org/10.1103/PhysRevE.89.052203.
- [16] L. Amarsid, J.Y. Delenne, P. Mutabaruka, Y. Monerie, F. Perales, F. Radjai, Viscoinertial regime of immersed granular flows, Phys. Rev. E 96 (2017)https://doi.org/10.1103/ PhysRevE.96.012901.
- [17] F. Pignatel, C. Asselin, L. Krieger, I.C. Christov, J.M. Ottino, R.M. Lueptow, Parameters and scalings for dry and immersed granular flowing layers in rotating tumblers, Phys. Rev. E Stat. Nonlin. Soft Matt. Phys. 86 (2012) 1–12, https://doi.org/10.1103/ PhysRevE.86.011304.
- [18] S.H. Chou, S.S. Hsiau, Dynamic properties of immersed granular matter in different flow regimes in a rotating drum, Powder Technol. 226 (2012) 99–106, https://doi. org/10.1016/j.powtec.2012.04.024.
- [19] H. Gayvallet, J.-C. Géminard, Ageing of the avalanche angle in immersed granular matter, Eur. Phys. J. B Condens. Matter. 30 (2002) 369–375, https://doi.org/10. 1140/epjb/e2002-00391-6.

- [20] D. Doppler, P. Gondret, T. Loiseleux, S. Meyer, M. Rabaud, Relaxation dynamics of water-immersed granular avalanches, J. Fluid Mech. 577 (2007) 161–181, https://doi.org/10.1017/S0022112007004697.
- [21] G. Varas, V. Vidal, J.C. Géminard, Dynamics of crater formations in immersed granular materials, Phys. Rev. E Stat. Nonlin. Soft Matt. Phys. 79 (2009) 1–7, https://doi.org/10.1103/PhysRevE.79.021301.
- [22] E. Grimaldi, E. Dressaire, Crater formation by sphere impact on a submerged granular bed, J. Vis. 19 (2016) 577–579, https://doi.org/10.1007/s12650-016-0353-y.
- [23] J. Koivisto, M. Korhonen, M. Alava, C.P. Ortiz, D.J. Durian, A. Puisto, Friction controls even submerged granular flows, Soft Matter 13 (2017) 7657–7664, https://doi.org/ 10.1039/c7sm00806f.
- [24] J. Koivisto, D.J. Durian, The sands of time run faster near the end, Nat. Commun. 8 (2017) 1–6, https://doi.org/10.1038/ncomms15551.
- [25] J. Fan, L.-H. Luu, G. Noury, P. Philippe, DEM-LBM numerical modeling of submerged cohesive granular discharges, Granul. Matter 22 (2020) 66, https://doi.org/10.1007/ s10035-020-01035-9.
- [26] A. Avagyan, D. Chiao, N. Dostart, K. Zhu, S. Cho, K. Remick, A.F. Vakakis, D.M. McFarland, W.M. Kriven, Experimental study of embedded and non-embedded ordered granular chains under impulsive excitation, Acta Mech. 227 (2016) 2511–2527, https://doi.org/10.1007/s00707-016-1564-y.
- [27] H. Kocharyan, N. Karanjgaokar, Influence of lateral constraints on wave propagation in finite granular crystals, J. Appl. Mech. 87 (2020)https://doi.org/10.1115/1. 4047004
- [28] N. Karanjgaokar, Evaluation of energy contributions using inter-particle forces in granular materials under impact loading, Granul. Matter 19 (2017) 36, https://doi. org/10.1007/s10035-017-0720-y.
- [29] A.I. Potapov, I.S. Pavlov, K.A. Gorshkov, G.A. Maugin, Nonlinear interactions of solitary waves in a 2D lattice, Wave Motion 34 (2001) 83–96, https://doi.org/10.1016/S0165-2125(01)00061-0.
- [30] V.F. Nesterenko, Dynamics of Heterogeneous Materials, 2001https://doi.org/10. 1007/978-1-4757-3524-6.
- [31] B. Andreotti, Y. Forterre, O. Pouliquen, Granular Media: Between Fluid and Solid, Cambridge University Press, 2013.
- [32] R.G. Cox, The motion of long slender bodies in a viscous fluid part 1. General theory, J. Fluid Mech. 44 (1970) 791, https://doi.org/10.1017/S002211207000215X.
- [33] B. Allen, A. Kudrolli, Effective drag of a rod in fluid-saturated granular beds, Phys. Rev. E 100 (2019), 022901, https://doi.org/10.1103/PhysRevE.100.022901.
- [34] T. Hossain, P. Rognon, Drag force in immersed granular materials, Phys. Rev. Fluids. 5 (2020), 054306, https://doi.org/10.1103/PhysRevFluids.5.054306.